

Optically heterodyne diagnosis of a high-saturation-power undoped InP sandwiched InGaAs p-i-n photodiode grown on GaAs

Yu-Sheng Liao, Jin-Wei Shi¹, Y.-S. Wu¹, Hao-Chung Kuo, M. Feng², and Gong-Ru Lin*

*Department of Photonics & Institute of Electro-Optical Engineering, National Chiao Tung University
Hsinchu, Taiwan 300, Republic of China*

grlin@faculty.nctu.edu.tw

¹*Department of Electrical Engineering, National Central University
Taoyuan, Taiwan 320, R.O.C.*

²*Department of Electrical and Computer Engineering, University of Illinois at Urbana-Champaign
Urbana, IL 61801, USA*

Abstract: We demonstrate the optical heterodyne diagnostics and high saturation power characteristics of a novel undoped InP sandwiched In_{0.53}Ga_{0.47}As p-i-n photodiode with a partially p-doped photoabsorption layer, which is grown on a linearly graded metamorphic In_xGa_{1-x}P buffered GaAs substrate layer and exhibits an excellent low dark current density of 3.6×10^{-7} A/cm². Such a top-illuminated optical receiver exhibits an illuminating window of 60- μ m diameter, which performs ultra-linear power handling capability up to 18 dBm at 1550 nm, providing a maximum photocurrent of 35 mA under a reverse bias of 9 volts. These result in extremely high current bandwidth and bandwidth-responsivity products of 350 mA•GHz and 4.8 GHz•A/W, respectively, at receiving frequency of up to 10 GHz.

©2006 Optical Society of America

OCIS codes: (040.5160) Photodetectors; (160 1890) Detector materials; (1201280) Detection; (060.2380) Fiber optics sources and detectors.

References

1. H. Ito, S. Kodama, Y. Muramoto, T. Furuta, T. Nagatsuma, T. Ishibashi, "High-Speed and High-Output InP-InGaAs Unitraveling-Carrier Photodiodes," *IEEE J. Sel. Top. Quantum Electron.* **10**, 709-727, (2004).
2. S. Demiguel, N. Li, X. Li, X. Zheng, J. Kim, J. C. Campbell, H. Lu, and A. Anselm, "Very High-Responsivity Evanescently Coupled Photodiodes Integrating a Short Planar Multimode Waveguide for High-Speed Applications," *IEEE Photon. Technol. Lett.* **15**, 1761-1763, (2003).
3. X. Li, N. Li, S. Demiguel, X. Zheng, J. C. Campbell, H. H. Tan, and C. Jagadish, "A Partially Depleted Absorber Photodiode With Graded Doping Injection Regions," *IEEE Photon. Technol. Lett.* **16**, 2326-2328, (2004).
4. V. Hurm, W. Benz, W. Bronner, M. Dammann, T. Jakobus, G. Kaufel, K. Kohler, Z. Lao, M. Ludwig, B. Raynor, J. Rosenzweig, M. Schlechtweg, "10 Gbit/s long wavelength pin-HEMT photoreceiver grown on GaAs," *Electron. Lett.* **33**, 1653-1654, (1994).
5. M. Zaknune, M. Ardouin, Y. Cordier, S. Bollaert, B. Bonte, and D. Théron, "60-GHz high power performance In_{0.35}Al_{0.65}As-In_{0.35}Ga_{0.65}As metamorphic HEMTs on GaAs," *Electron. Lett.* **36**, 741-742, (2003).
6. M. V. Maksimov, Yu. M. Shernyakov, N. V. Kryzhanovskaya, A. G. Gladyshev, Yu. G. Musikhin, N. N. Ledentsov, A. E. Zhukov, A. P. Vasil'ev, A. R. Kovsh, S. S. Mikhlin, E. S. Semenova, N. A. Maleev, E. V. Nikitina, V. M. Ustinov, and Zh. I. Alferov, "High-power 1.5 μ m InAs-InGaAs quantum dot lasers on GaAs substrates," *Semiconductors* **38**, 732-735, (2004).
7. M. Chertouk, H. Heiss, D. Xu, S. Kraus, W. Klein, G. Böhm, G. Tränkle, and G. Weimann, "Metamorphic InAlAs/InGaAs HEMT's on GaAs substrates with a novel composite channels design," *IEEE Electron. Device Lett.* **17**, 273-275, (1996).
8. K. L. Averett, X. Wu, M. W. Koch, and G. W. Wicks, "Low-voltage InAsP/InAs HBT and metamorphic InAs BJT devices grown by molecular beam epitaxy," *J. Cryst. Growth* **251**, 852-857, (2003).
9. J.-H. Jang, G. Cueva, W. E. Hoke, P. J. Lemonias, P. Fay, and I. Adesida, "Metamorphic Graded Bandgap InGaAs-InGaAlAs-InAlAs Double Heterojunction P-i-I-N Photodiodes," *J. Lightwave Technol.* **20**, 507-514, (2002).

10. C.-K. Lin, H.-C. Kuo, M. Feng, G.-R. Lin, "Ultralow Leakage In_{0.53}Ga_{0.47}As p-i-n Photodetector Grown on Linearly Graded Metamorphic In_xGa_{1-x}P Buffered GaAs Substrate," *IEEE J. Quantum Electron.* **41**, 749-752, (2005).
 11. K. J. Williams and R. D. Esman, "Large-signal Compression-current Measurements in High-power Microwave pin Photodiodes," *Electron. Lett.*, **35**, 82-84, (1999).
 12. Y.-S. Wu, J.-W. Shi, J.-Y. Wu, F.-H. Huang, Y.-J. Chan, Y.-L. Huang, and R. Xuan, "High-Performance Evanescently Edge Coupled Photodiodes With Partially p-Doped Photoabsorption Layer at 1.55- μ m Wavelength," *IEEE Photon. Technol. Lett.* **17**, 878-880, (2005).
 13. F. Xia, J. K. Thomson, M. R. Gokhale, P. V. Studenkov, J. Wei, W. Lin, and S. R. Forrest, "A asymmetric twin-waveguide high-bandwidth photodiode using a lateral taper coupler," *IEEE Photon. Technol. Lett.*, vol. 13, no. 8, pp. 845-847, Aug. 2001.
 14. S. Kawanishi, M. Saruwatari, "A very wide-band frequency response measurement system using optical heterodyne detection", *IEEE Trans. Instrum. Meas.* **38**, 569 - 573, (1989).
 15. Z. Griffith, Y.-M. Kim, M. Dahlström, A. C. Gossard, and M. J. W. Rodwell, "InGaAs-InP Metamorphic DHBTs Grown on GaAs With Lattice-Matched Device Performance and $f_{max} > 268$ GHz," *IEEE Electron. Lett.* **25**, 675-677, (2004).
 16. G.-R. Lin, I.-H. Chiu, and M.-C. Wu, "1.2-ps mode-locked semiconductor optical amplifier fiber laser pulses generated by 60-ps backward dark-optical comb injection and soliton compression," *Opt. Express* **13**, 1008-1014, (2005).
-

1. Introduction

InP-based high-speed optoelectronic devices [1-3] and integrated circuits (OEICs) [4-5] have been comprehensively investigated in long-wavelength (from 1.1 to 1.65 μ m) fiber-optic communication networks. Recently, different metamorphic (MM) epitaxial layers such as InGaAs [6], InAlAs [7], InAs [8], InGaAlAs [9], and InGaP [10] etc. have emerged as the buffer layers for growing InGaAs-based optoelectronic devices on GaAs substrates with lower process cost. Compositionally graded metamorphic buffer layers are extensively utilized to accommodate large lattice mismatch between a semiconductor substrate and epitaxial layers, which overcomes the limitation of band-gap engineering imposed by the substrate lattice parameters. Technically, the metamorphic epitaxy facilitates some advantages of improved mechanical strength, ready availability of larger diameter substrates than InP, easier material handling, process robustness, and the compatibility with the existing manufacturing infrastructure. In general, photodiodes made of narrow-band gap materials are operated under zero bias because of their high leakage current and low breakdown voltage. Infrared diodes are selected according to the resistance and area (RoA) product. However, the RoA product is degraded by increase in current leakage. Thus, there is interest in investigating low-leakage photodetectors with high modulation frequency. Recently, most advancements in high-data-rate optical communications system have focused on increasing the bandwidth and output voltage of photodetectors (PDs) in order to eliminate the need for postdetection amplification and instead directly drive the decision making circuitry. In digital fiber-optic systems, the PDs with high sensitivities are usually placed after an erbium-doped-fiber-amplifier or semiconductor optical amplifier. The new approach becomes attractive when high-saturation-current photodiodes are available, so that the output from the photodiode can directly drive a decision circuit. High optical wide-band-width PDs designed to achieve these output power continue to be elusive.

Several high-power and surface-illuminated InP-InGaAs PDs have been demonstrated with small-signal photocurrent of 30 mA at 20 GHz and 48 mA at 10 GHz [11]. In this paper, we report for the fabrication of top-illuminated metamorphic p-i-n photodiodes (MM-PINPD) with partially p-doped photoabsorption layer [3, 12] on GaAs substrates using linearly graded In_xGa_{1-x}P buffer layer. We incorporated the partially p-doped photoabsorption layer and metamorphic structure to get a good balance of its electronic bandwidth, the capability of radio-frequency (RF) power generation, and cost-effective consideration. The MM-PINPD has the graded partially p-doped photoabsorption layer to accelerate the drift velocity of the photo-excited electrons, since the bandwidth of our previous structure [10] was not transit-

time limited. In this letter, we had modified the structure with partially p-doped photoabsorption layer. Compared to our previous work, the new structure demonstrated nearly the higher saturation current and higher bandwidth of 8 GHz without sacrificing the responsivity. The demonstrated metamorphic epitaxy is particularly suitable for mass-production of such devices on GaAs substrates. Ultralow leakage current, high operating bandwidth and high saturation current product performances have been achieved simultaneously. By using such a metamorphic buffer and partial p-doping, an InGaAs PINPD with a very low dark current density, high operating bandwidth, and high saturation current product was reported. These results interpret the capability of such a device for application in a 10Gbit/s SONET/SDH networks or a 5-GHz radio-over-fiber systems.

2. Experimental setup

Prior to the growth of InGaAs MM-PINPD structure, a 1.5 μm -thick linearly graded metamorphic $\text{In}_x\text{Ga}_{1-x}\text{P}$ buffer layer with x gradually changing from 0.49 to 1 was deposited on a 3-in (100)-oriented semi-insulating (SI) GaAs by using gas source molecular beam epitaxy (GSMBE) at substrate temperature of 500°C. An InGaAs MM-PINPD was subsequently grown at 600°C, which consists of 1 μm -thick n+-InP, 0.5 μm -thick undoped InP, 2.5 μm -thick undoped $\text{In}_{0.53}\text{Ga}_{0.47}\text{As}$, and 1 μm -thick graded doping p-InP (after Zn diffusion) layers as shown in Fig. 1. After epitaxy, the coplanar guard-ring typed ground-signal-ground contact electrodes with circular window diameter of 60 μm , two n-type ground contact pads and one central p-type contact pad are fabricated by evaporating 800 nm-thick Ni/Au and Ti/Au metals, respectively. This design facilitates the diagnostics of the InGaAs MM-PINPD by a lightwave probe station with a 65-GHz coplanar-waveguide typed millimeter-wave probe (Picoprobe 65A-GSG-70-P) as shown in the Fig. 2. The composition, structural quality and the degree of strain relaxation were subsequently evaluated by high-resolution x-ray diffraction and the cross-section transmission electron microscopy (TEM), which shows a defect density as low as $6 \times 10^6 \text{ cm}^{-2}$ in the linearly-graded $\text{In}_x\text{Ga}_{1-x}\text{P}$ metamorphic buffer layer.

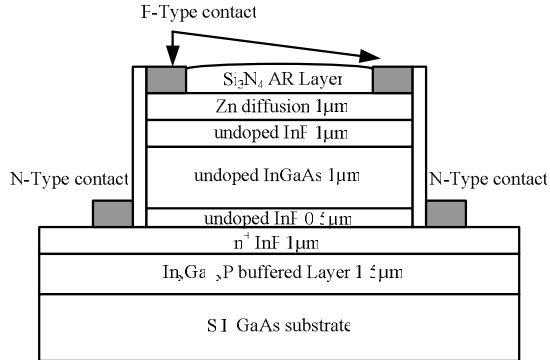


Fig. 1. Configuration of the InGaAs MM-PINPD on semi-insulating GaAs substrate.



Fig. 2. Top-view photograph of the InGaAs MM-PINPD

The bandwidth and saturation current were measured with a heterodyne beating [13, 14] setup as shown in Fig. 3. The heterodyne beating photocurrent of a MM-PINPD is given by $i_c(t) = \frac{e\eta}{hv} \left\{ I_1 + I_2 + 2 \cos \theta \cdot F(\omega_b) \sqrt{I_1 I_2} \cos(\omega_b t) \right\}$, where I_1 and I_2 are the received optical intensities of two tunable lasers with a frequency difference ω_b , θ is the angle between the polarization directions of lasers, e is the electron charge, η is quantum efficiency, $h\nu$ is the photon energy, and $F(\omega_b)$ is the frequency response of the MM-PINPD. The spectral power of $P(\omega_b) = 2 \left(\frac{e\eta}{hv} \right)^2 I_1 I_2 R_L \cos^2 \theta \cdot F^2(\omega_b) \arctan \left(\frac{2\pi B}{\Delta\omega} \right)$ is obtained, where R_L is the input

impedance of the spectrum analyzer, B is the resolution bandwidth of the spectrum analyzer, and $\Delta\omega$ is the linewidth (FWHM) of the beating signal.

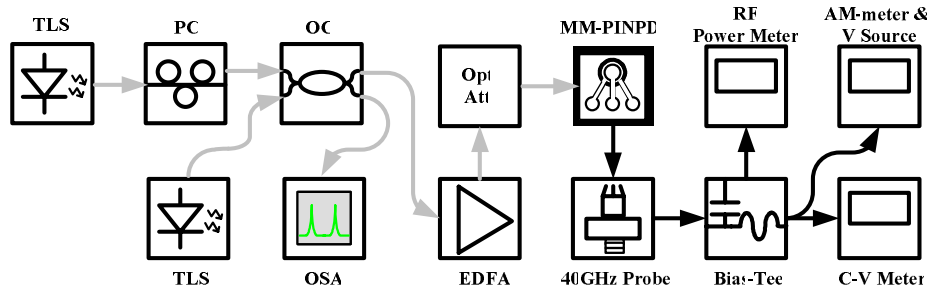


Fig. 3. Setup of the heterodyne beating measurement for the coplanar guard-ring typed InGaAs PINPD. PC: polarization controller, Opt. Att.: optical attenuator, TLS: tunable laser source, OSA: optical spectrum analyzer.

3. Results and discussion

The structure of InGaAs MM-PINPD is similar as previous reports except the whole structure was grown on semi-insulating substrate [15]. The metamorphic buffer absorbs the strain of lattice mismatch and prevents the vertical propagation of dislocations, thereby maintaining the quality of the device active layers. The dark current of the MM-PINPD on GaAs substrate is an effective measurement of the quality of the metamorphic buffer layer. The dark currents of photodiodes were highly dependent upon the metamorphic buffer layer. The continuously graded buffer layer provides lower dark currents, with a buffer structure in which indium and gallium concentrations are ramped inversely. A thick InGaP buffer layer can generate a high density of defects that results in high dark currents because of the unfiltered lattice-mismatch strain and the difference in thermal expansion coefficients between InGaP and the GaAs substrate. Therefore, the magnitude of dark currents could reflect the quality of InGaP metamorphic layer. The I-V responses under 1550-nm CW light: (a) 0 dBm, (b) -20 dBm, (c) -40 dBm, (d) -60 dBm, (e) -80 dBm, (f) dark current of the negatively biased MM-PINPD with 60- μm diameter is plotted in Fig. 4. Even with the metamorphic layer, an extremely low dark current of 13 pA is obtained at a bias voltage of -5 V, as shown in Fig. 5. Such a leakage current density is almost three orders of magnitude lower than the previously reported InGaAs MM-PINPD made on GaAs with a different metamorphic buffer layer, which reveals the improvement in lattice grading property between InGaAs layer and GaAs substrate with the adding of metamorphic InGaP buffer.

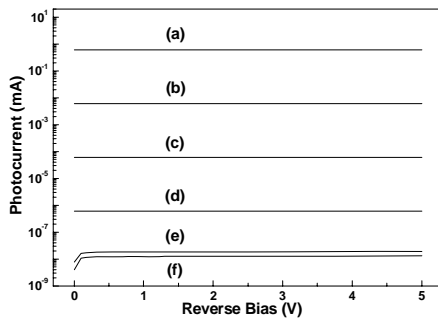


Fig. 4. Photocurrent of MM-PINPD at (a) 0 dBm, (b) -20 dBm, (c) -40 dBm, (d) -60 dBm, and (e) -80 dBm

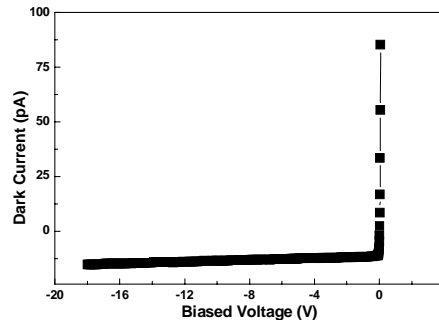


Fig. 5. Dark current versus biased voltage from 0.1 V to -18 V for MM-PINPD

In previous works, versatile compositionally graded metamorphic buffer layers are extensively utilized to confine threading dislocations and defects in the metamorphic InGaP

buffer without propagating vertically into the device layer. The InP layer can be very smooth since there is no compositional control problem in the InGaP/InP system. Furthermore, since the bandgap of InGaP is larger than that of InP, a fully transparent buffer layer can be achieved. The TEM analysis and the ultra-low dark current of the MM-PINPD also reveals the device layers upon the metamorphic buffer which are nearly dislocation-free (with density of $1 \times 10^6 \text{ cm}^{-2}$). The InP-InGaAs-InP layer with sandwiched structure leads to broad equivalent width of InGaAs, and this structure is suitable for high-voltage and high electric-field operation. Carriers are trapped at the sandwiched structure which results in ultralow dark current due to the higher band gap of InP than that of InGaAs. Figure 6 shows a energy-band diagram of the MM-PINPD at a reverse bias 5 V. Such a excellent low dark current density of $3.6 \times 10^{-7} \text{ A/cm}^2$ not only reveals the better lattice-matching property between the InGaP buffer and the GaAs substrate, but also gives to a minimum detectable power of below 100 pW. These results again reflect that reducing the leakage current is a decisive way to improve the sensitivity of the MM-PINPD owing to the significant suppression on noise equivalent power of the receiver module. The shot and thermal noises of the MM-PINPD without a matching circuit are calculated as $6.9 \times 10^{-11} \text{ A}$ and $1.1 \times 10^{-12} \text{ A}$, respectively.

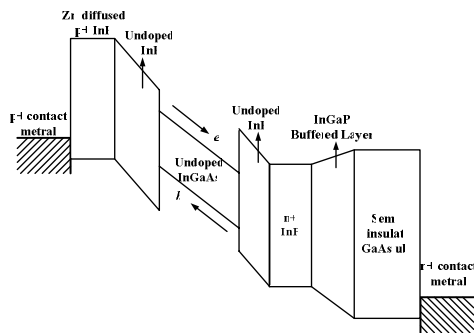


Fig. 6. Band diagram of the MM-PINPD at reversed bias 5 V.

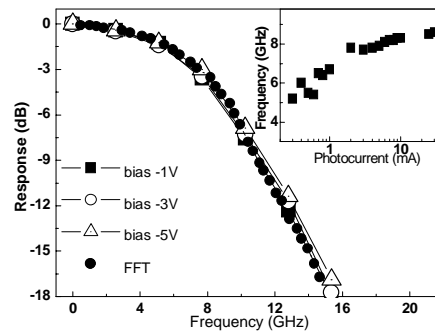


Fig. 7. Frequency responses at reverse biases of -1V, -3V, and -5V. The FFT response obtained from impulse method is shown for comparison. The inset shows the illumination power dependent 3-dB frequency response as a function of photocurrent.

For a reverse biased MM-PINPD, it is important to minimize the leakage and obtain high frequency response concurrently. The transit time of carriers can be shortened by reducing the thickness of the absorption layer, reducing the device leakage current and obtaining a high-speed response. However, reducing the absorption layer thickness of the absorption usually lead to a lower quantum efficiency. The photocurrent of the MM-PINPD measured at a reverse bias of 5 V is 0.6 mA, under an illuminating power of 0 dBm, corresponding to an optical responsivity of 0.6 A/W which indicates that the p-doped photoabsorption layer of our structure does not sacrifice the performance of our quantum efficiency. In order to further study the speed and power performances of the MM-PINPD, the frequency response of a 60- μm -diameter PD was measured under different biases, as shown in Fig. 7. The inset of Fig. 7 shows that the 3-dB frequency response is increased as the photocurrent enlarges from 0.2 to 30 mA, in which a saturating effect on the bandwidth enhancement can be seen at photocurrent $> 2 \text{ mA}$. One can clearly see that under bias from -1 to -5 V, the MM-PINPD exhibits a 3-dB bandwidth of 8.3 GHz under a 30-mA output condition. In principle, the bandwidth enhancement is due to a reduction in the transit time across the doped absorbing layers, which arises from the increase of minority carrier based drift current and the presence of high photocurrent in the active layer. The frequency response was also verified by using impulse response. The mode-locked semiconductor optical amplifier (SOA) fiber laser [16] with a full width at half maximum (FWHM) of 1.2 ps was served as an input source. The

impulse response of the MM-PINPD reveals a FWHM of 40 ps, which indicates the bandwidth of 8 GHz from the fast Fourier transform. The bandwidth-responsivity product of 4.8 GHz•A/W of proposed MM-PINPD was measured. In comparison, a 32- μm diameter commercial PINPD (Emcore, InGaA/InP PINPD, model 8413-1155) obtains the dark current density of 6.2×10^{-5} A/cm² at a bias of -3.5 V and our proposed MM-PINPD exhibits better performance of dark current density than this commercial InGaA/InP PINPD. Besides, Jang *et al.* have previously demonstrated a MM-PINPD with a p⁺-InGaAs/InGaAs/n⁺-InAlAs p-i-n structure on a linearly graded InAlGaAs buffer layer [9], in which the In_{1-x-y}Ga_xAl_yAs layer serves as a lattice-constant transformer between the GaAs substrate and the In_{0.53}Ga_{0.47}As layers with a low dark current density of 3.4×10^{-4} A/cm² at bias of -5 V and an optical responsivity of 0.6 A/W at 1.55 μm was reported. The used photo-absorption-layer thickness of the reported device is 3.6 times larger than that of device in Ref. [9] (2.5 μm vs. 0.7 μm). For fair comparison, the dark current and dark current density under -18 V bias, which in order to meet the same electric field in the InGaAs layer, was measured as 15.5 pA and 4.3×10^{-7} A/cm². Such a leakage current density is almost three orders of magnitude lower than the compared one. Although the compared metamorphic PD can have 0.6 A/W responsivity with an electrical bandwidth of 38 GHz, such small 10 μm diameter of PD shows RC time limited bandwidth but sacrifice the stability of coupling.

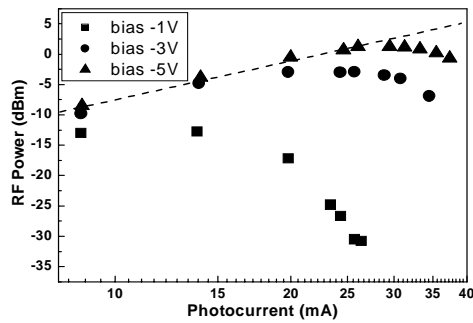


Fig. 8. RF power versus photocurrent under the reversed bias of 1, 3, 5 V at a operating frequency of 10 GHz.

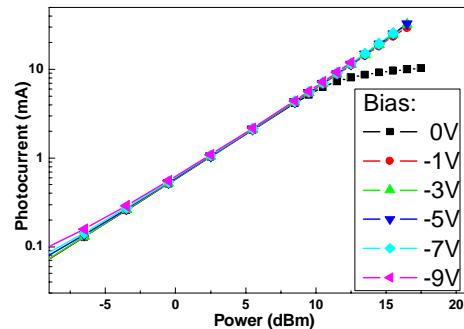


Fig. 9. The dc saturation characteristic of the MM-PINPD.

The RF power of the MM-PINPD under different bias voltages at operating frequency of 10 GHz and the saturation characteristic was illustrated in Fig. 8. A 60- μm -diameter top-illuminated photodiode is shown to exhibit optical responsivities of 0.77 A/W and 0.6 A/W at 1310 nm and 1550 nm, respectively, achieving a saturated photocurrent of 35 mA at the bandwidth of 10GHz. The current-bandwidth product of our MMPIN-PD was measured as 350 mA•GHz. The ideal relation between the RF power of 100% modulated large signal and the average current on a 50-ohm load is also plotted as a straight line for reference. The demonstrated maximum values of the generated RF power and the averaged photocurrent of the device were limited by the device failure under high current operation. The maximum RF power of 1 dBm and photocurrent of 35 mA can be respectively obtained, and the values were higher than those reported in previous work on top-illuminated p-i-n photodetectors with such low leakage current. For the case of high-speed PDs, there is a significant trade-off between saturation current and electrical bandwidth. Previously, Li *et al.* have demonstrated a partially depleted absorber photodiode with a saturation current bandwidth product of 990 mA•GHz and a responsivity of 0.67 A/W [3]. Under backside illumination at 1.55- μm wavelength, an 8- μm -diameter photodiode exhibited an increase in bandwidth with increasing photocurrent. These measurement results indicate that the technique of partially p-doped photoabsorption layer enhance the speed and output power performance of photocurrent significantly without sacrificing the device performance. The p-doped region can shorten the

depletion width of the photoabsorption layer, reduce the space charge field of photo-excited carriers, and increase the output saturation current effectively. The photo generation of holes in the intrinsic layer of the MM-PINPD can result in larger space charge effects than those in the structure. However, this effect is not as severe if the drift layer is thin. The total induced potential gradient is higher than efficient potential gradient, which results from the graded doping. Since potential gradients induced by doping and input power are independent of each other. The average electric field is higher than the small photocurrent case. Therefore, the transit time of electrons in the p-doped region is decreased and the bandwidth is enhanced. The layers of InP-InGaAs-InP with sandwiched structure leads to broaden equivalent energy gap of InGaAs, which can be obtained in high electrical field. For these reasons, the MM-PINPD can be operated under low bias voltage to reduce the total power consumption, while still suppressing saturation. Furthermore, as compared to less thickness of intrinsic InGaAs photoabsorption layer, this technique on our MM-PINPD does not increase the device absorption length or sacrifice the responsivity. The obtained high electrical bandwidth under high photocurrent operation (around 10 GHz at 35 mA) of demonstrated device with a 60- μm -diameter and GaAs substrate ensure its applications to 10 Gbit/s analog and digital fiber communication systems.

5. Conclusion

The optical heterodyne diagnosis of a low-dark-current and high saturation power undoped InP sandwiched $\text{In}_{0.53}\text{Ga}_{0.47}\text{As}$ p-i-n photodiode with the partially p-doped photoabsorption layer on GaAs with linearly graded metamorphic $\text{In}_x\text{Ga}_{1-x}\text{P}$ buffer layer has been demonstrated. The low dark current of the photodetector demonstrated the high quality of the sandwiched InP-InGaAs-InP structure and proved the effectiveness of the metamorphic buffer layer. Such a state-of-the-art low dark current density of $3.6 \times 10^{-7} \text{ A/cm}^2$ not only reveals the better lattice-matching property between the InGaP buffer and the GaAs substrate, but also gives to a minimum detectable power of below 100 pW. The optical responsivities of 0.77 A/W and 0.6 A/W, and the NEP of $2.7 \times 10^{-15} \text{ W/Hz}^{1/2}$ and $3.4 \times 10^{-15} \text{ W/Hz}^{1/2}$, have been determined at 1310 nm and 1550 nm, respectively. Such a top-illuminated optical receiver exhibits an illuminating window of 60- μm diameter, which performs ultra-linear power handling capability up to 18 dBm at 1550 nm, providing a maximum photocurrent of 35 mA under a reverse bias of 9 volts. By utilizing the technique of partially p-doped photoabsorption layer, the demonstrated MM-PINPD has improvement in high-power performance without sacrificing its speed and responsivity performance, and optically heterodyne beating diagnosis the frequency characteristic of 3-dB bandwidth of 8 GHz and bandwidth-responsivity product of 4.8 GHz•A/W. These are the highest current-bandwidth product report made on metamorphic GaAs substrate, as high as 350 mA•GHz. The bandwidth enhancement effect due to adopt partially p-doped photoabsorption layer when the bandwidth of the photodiode were RC time limited. The overall characteristics of the device exhibited performance required for application in 10Gbit/s optical fiber communication or 5-GHz radio-over-fiber systems.

Acknowledgments

The authors thank the National Science Council of Republic of China for financially supporting this research under grant NSC94-2215-E-009-040.